

## Photochemistry of the $\text{IrCl}_6^{2-}$ complex in methanol matrices

E.M. Glebov<sup>a</sup>, V.F. Plyusnin<sup>a,\*</sup>, V.L. Vyazovkin<sup>a</sup>, A.B. Venediktov<sup>b</sup>

<sup>a</sup> Institute of Chemical Kinetics and Combustion SB RAS, 630090 Novosibirsk, Russia

<sup>b</sup> Institute of Inorganic Chemistry SB RAS, 630090 Novosibirsk, Russia

Received 27 November 1996; accepted 28 January 1997

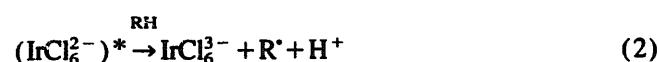
### Abstract

Low-temperature spectrophotometry and electron spin resonance (ESR) were used to study the  $\text{IrCl}_6^{2-}$  photochemistry in methanol matrices frozen at 77 K. Photoreaction gives rise to the absorption band of an  $\text{IrCl}_6^{3-}$  complex with a maximum at 215 nm and to a new band with a maximum at 287 nm that is unobservable during  $\text{IrCl}_6^{2-}$  photolysis in solutions at room temperature. The appearance of this new band is assigned to the formation of a weak complex between the  $\cdot\text{CH}_2\text{OH}$  radical and  $\text{IrCl}_6^{3-}$  ion (i.e. a  $\text{IrCl}_6^{3-} \dots \cdot\text{CH}_2\text{OH}$  radical complex). The irradiation of methanol matrix with  $\text{IrCl}_6^{2-}$  gives rise to the  $\cdot\text{CH}_2\text{OH}$  radical signal in the ESR spectrum with additional splitting which can be attributed to the partial delocalization of spin density from radical to the  $\text{IrCl}_6^{3-}$  complex and the appearance of hyperfine splitting (HFS) on the iridium nucleus. When the matrix is heated to 115 K the  $\text{IrCl}_6^{3-} \dots \cdot\text{CH}_2\text{OH}$  complex disappears. © 1997 Elsevier Science S.A.

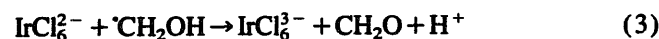
**Keywords:**  $\text{IrCl}_6^{2-}$ ; Methanol matrix; Photolysis; Optical spectroscopy; Electron spin resonance

### 1. Introduction

Stationary and laser flash photolysis have been used to demonstrate that in alcohol solutions at room temperature the  $\text{IrCl}_6^{2-}$  complex reduces to  $\text{IrCl}_6^{3-}$  under irradiation at 308 nm by the electron transfer from the solvent to the excited complex [1]:



The quantum yield for methanol solutions is 0.1. The solvent radical ( $\cdot\text{CH}_2\text{OH}$  for methanol) reacts with the initial  $\text{IrCl}_6^{2-}$  complex:



with the rate constant  $3.2 \times 10^9 \text{ M}^{-1} \text{ s}^{-1}$ . A similar primary mechanism of phototransformations is realized in the photochemistry of halide complexes of Fe(III) [2–4], Cu(II) [5–7] and Pt(IV) [8–10] in organic solvents. The photolysis of  $\text{CuCl}_4^{2-}$  complexes in frozen organic matrices gives rise to optical absorption bands and the ESR spectrum of  $\text{CuCl}_4^{2-} \dots \text{R}^\cdot$  radical complex [5–7]. Laser flash photolysis of  $\text{PtCl}_6^{2-}$  methanol solutions at low temperatures (160–220 K) shows that in this case the primary species is also the

radical complex  $\text{PtCl}_6^{3-} \dots \text{R}^\cdot$  [8–10]. The formation of the intermediate radical complex  $\text{Mo(V)} \dots \text{R}$  has also been recorded in the photolysis of Mo(VI) oxocomplexes in alcohol matrices [11].

The identity of the primary photoprocesses for  $\text{IrCl}_6^{2-}$  and chloride complexes of Fe(III), Cu(II) and Pt(IV) suggests the possible formation of the intermediate short-lived radical complex in the case of  $\text{IrCl}_6^{2-}$  photochemistry. The goal of the present contribution was to search for the spectral evidence of the  $\text{IrCl}_6^{3-} \dots \text{R}^\cdot$  complex in the frozen methanol matrix.

### 2. Experimental details

The salt  $\text{Na}_2\text{IrCl}_6 \cdot 6\text{H}_2\text{O}$  was synthesized as described in Ref. [12] and used to prepare the solutions of  $\text{IrCl}_6^{2-}$  complex. Solutions of  $\text{IrCl}_6^{2-}$  complex were prepared using the salt  $\text{Na}_3\text{IrCl}_6 \cdot \text{H}_2\text{O}$  (Aldrich Chem. Co.). Methanol with 10 vol.% of water was used as a solvent to obtain glassy methanol matrices. When necessary, oxygen was removed from solutions by pumping and repeated freezing of solutions at the temperature of liquid nitrogen (77 K).

Stationary photolysis was performed using radiation from an excimer XeCl (308 nm) laser or a high-pressure mercury lamp using glass filters to distinguish the necessary spectral lines. Optical spectra were recorded on a Spex UV-visible

\* Corresponding author. Tel: +7 3832 357061; fax: +7 3832 352350.

spectrophotometer (Carl Zeiss). For details of the low-temperature photochemical experimental technique see Ref. [13]. ESR spectra were recorded using a "Sibir" spectrometer with further processing on an IBM computer. Radiolysis was performed using a  $^{60}\text{Co}$  source. The trapped electrons were removed by irradiating the sample with red light. To quantitatively compare the data obtained by the methods of low-temperature spectrophotometry and ESR, the corresponding spectra were recorded using the same sample [13].

### 3. Results and discussion

#### 3.1. $\text{IrCl}_6^{2-}$ photolysis in methanol matrix

The optical spectrum of the  $\text{IrCl}_6^{2-}$  complex [14,15] contains charge transfer bands in the UV ( $\lambda = 232$  nm,  $\epsilon = 20\,900\text{ M}^{-1}\text{ cm}^{-1}$ ) and visible spectrum regions ( $\lambda = 430, 450$  ( $\epsilon = 3000\text{ M}^{-1}\text{ cm}^{-1}$ ), and at 495 nm ( $\epsilon = 4000\text{ M}^{-1}\text{ cm}^{-1}$ )). The weaker d-d bands are located in the regions 306, 360, and 530 nm ( $\epsilon \approx 1000\text{ M}^{-1}\text{ cm}^{-1}$ ). As the solution temperature is decreased, the positions of the absorption band maxima remain invariant, although their width decreases and the extinction coefficient increases. Thus, for example, the extinction coefficient of the band with maximum at 495 nm increases from  $4000\text{ M}^{-1}\text{ cm}^{-1}$  at 293 K to  $5800\text{ M}^{-1}\text{ cm}^{-1}$  at 77 K.

When photolysis is performed in methanol matrices, the disappearance of the  $\text{IrCl}_6^{2-}$  optical spectrum gives rise to new absorption bands with maxima at 215 and 287 nm ( $46\,510$  and  $34\,840\text{ cm}^{-1}$ ) preserving three isosbestic points at 223, 277, and 306 nm (Fig. 1). For methanol matrices the quantum yield of  $\text{IrCl}_6^{2-}$  disappearance is 0.03 (measurement accuracy to within 10%).

Photolysis of  $\text{IrCl}_6^{2-}$  in methanol solutions at room temperature leads to the appearance of an  $\text{IrCl}_6^{3-}$  complex absorption band with a maximum at 209 nm [1]. Under irradiation, the isosbestic point is preserved at 223 nm, which allows a determination of the extinction coefficient of this band as  $28\,500\text{ M}^{-1}\text{ cm}^{-1}$ . When the  $\text{Na}_3\text{IrCl}_6$  salt is dissolved in methanol, the  $\text{IrCl}_6^{3-}$  complex absorption band displays a maximum at 209 nm with an extinction coefficient of  $28\,500\text{ M}^{-1}\text{ cm}^{-1}$ . If the  $\text{Na}_3\text{IrCl}_6$  solutions are frozen in methanol at 77 K, the absorption band maximum of the  $\text{IrCl}_6^{3-}$  complex shifts to 211 nm and its extinction coefficient is  $25\,000\text{ M}^{-1}\text{ cm}^{-1}$ . The effective extinction coefficient of the band at 215 nm arising from  $\text{IrCl}_6^{2-}$  photolysis in methanol matrix is  $19\,000\text{ M}^{-1}\text{ cm}^{-1}$ . Thus, both the position of the maximum and the extinction coefficient of a shortwave band arising from  $\text{IrCl}_6^{2-}$  photolysis in methanol matrix are close to the values typical of the  $\text{IrCl}_6^{3-}$  complex obtained by either the dissolving of  $\text{Na}_3\text{IrCl}_6$  or the photoreduction of  $\text{IrCl}_6^{2-}$  at room temperature.

The second band with a maximum at 287 nm (Fig. 1) does not belong to the  $\text{IrCl}_6^{3-}$  complex because it appears only under  $\text{IrCl}_6^{2-}$  photolysis in the frozen matrix. A solvent rad-

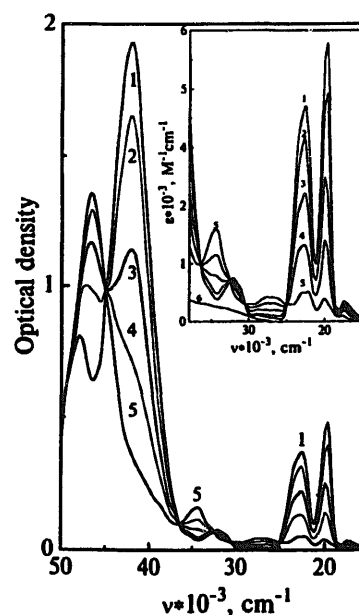


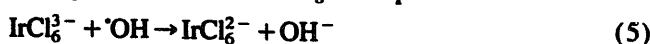
Fig. 1. Change in the optical spectrum of  $\text{IrCl}_6^{2-}$  complex ( $8.3 \times 10^{-3}\text{ M}$ ) in methanol matrix (77 K) in photolysis at 308 nm (cuvette thickness, 0.01 cm; laser pulse energy, 3 mJ; pulse repetition frequency, 10 Hz). Curves 1–5 denote 0, 1, 4.5, 9, and 19 min of irradiation, respectively. The inset shows the spectrum region at a larger scale with extinction coefficient along the ordinate. Curve 6 in the inset is the  $\text{CH}_2\text{OH}$  radical spectrum taken from [18].

ical forms from the photoreduction of the chloride complexes of transient metals in frozen matrices [16]. For methanol matrices, this is the  $\text{CH}_2\text{OH}$  radical [17]. However, the band at 287 nm cannot belong to the  $\text{CH}_2\text{OH}$  radical because it is inconsistent with the optical absorption of this particle determined experimentally from pulsed radiolysis of methanol [18,19]. Fig. 1 (spectrum 6 in the inset) depicts the optical spectrum of  $\text{CH}_2\text{OH}$  radical taken from Ref. [18]. Thus, the band at 287 nm does not belong either to the  $\text{IrCl}_6^{3-}$  complex or to the  $\text{CH}_2\text{OH}$  radical.

Broszkiewicz [20] demonstrated the formation of an intermediate absorption band with a maximum at 280 nm and an extinction coefficient of  $1700\text{ M}^{-1}\text{ cm}^{-1}$  for pulsed radiolysis of  $\text{IrCl}_6^{2-}$  in aqueous solution containing 0.1 M *t*-butanol. This band has been assigned to the  $\text{IrCl}_6^{4-}$  complex arising from the reaction of  $\text{IrCl}_6^{3-}$  with an aquated electron

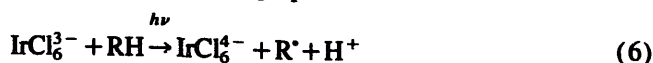


However, this band was recorded only in the presence of *t*-butanol. It is assumed then that in the aqueous solution containing no *t*-butanol, the  $\text{IrCl}_6^{2-}$  complex forms



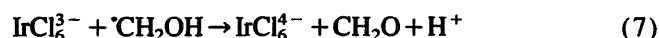
The absorption of  $\text{IrCl}_6^{2-}$  masks the  $\text{IrCl}_6^{4-}$  band. In the presence of *t*-butanol the  $\text{OH}$  radical rapidly converts into alcohol radical and  $\text{IrCl}_6^{2-}$  does not form.

In our case, the complex of bivalent iridium can result from the photolysis of  $\text{IrCl}_6^{2-}$  (reaction (6)) that is accumulated due to the primary  $\text{IrCl}_6^{2-}$  photoreduction



This has been verified by both the preparation of  $\text{Na}_3\text{IrCl}_6$  methanol solutions and the photolysis of  $\text{IrCl}_6^{2-}$  obtained photochemically in the liquid solution. However, even under the prolonged laser irradiation at 308 nm the optical spectrum of  $\text{IrCl}_6^{2-}$  does not vanish and the band at 287 nm does not form in the frozen matrix.

The second possible mechanism of formation of the bivalent iridium complex is either the dark or photochemical reaction of electron transfer from the solvent radical to the  $\text{IrCl}_6^{2-}$  complex, i.e. the reaction of particles arising in the primary process of  $\text{IrCl}_6^{2-}$  photoreduction that cannot part in the conditions of the rigid matrix



In this case, the appearance of band at 287 nm must cause the disappearance of the  $\text{}^1\text{CH}_2\text{OH}$  radical signal from the ESR spectrum. Further, we will consider the relation between the concentrations of radical particles recorded by the ESR method and quantity of photoreduced  $\text{IrCl}_6^{2-}$  complex.

### 3.2. ESR spectra of the products of $\text{IrCl}_6^{2-}$ photolysis in frozen matrices

The  $\text{IrCl}_6^{2-}$  complex is a paramagnetic ion (electron configuration  $5d^5$ , strong crystalline field, full electron spin  $1/2$ ). However, its ESR signal at 77 K is strong broadened due to spin-orbit interaction and a large anisotropic  $g$ -factor [21] and at concentrations of  $10^{-3}$ – $10^{-2}$  M its amplitude is small.

The primary product of  $\text{IrCl}_6^{2-}$  photolysis performed in the methanol matrix is the  $\text{}^1\text{CH}_2\text{OH}$  radical. The characteristic triplet of this radical (Fig. 2) arises in the ESR spectrum as soon as irradiation is started. For comparison, Fig. 2 depicts the ESR spectrum of this radical obtained by the  $\gamma$ -radiolysis

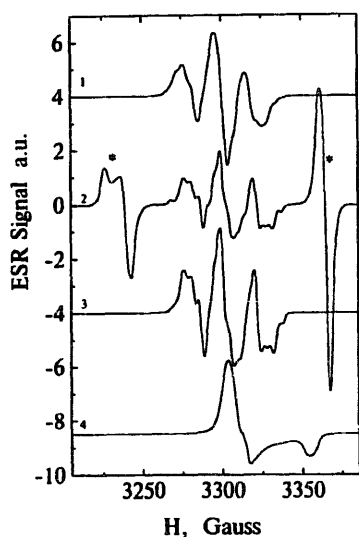


Fig. 2. ESR spectrum of  $\text{IrCl}_6^{2-}$  photolysis products in methanol matrix. Curve 1, ESR spectrum of  $\text{}^1\text{CH}_2\text{OH}$  radicals after  $\gamma$ -radiolysis of methanol matrix; curve 2, ESR spectrum after  $\text{IrCl}_6^{2-}$  photolysis in methanol matrix (the lines of  $\text{HCO}^\bullet$  radicals are asterisked); curve 3, ESR spectrum of  $\text{}^1\text{CH}_2\text{OH}$  radical (spectrum 2 after "light" annealing ( $\lambda > 530$  nm) of  $\text{HCO}^\bullet$  radical); curve 4, ESR spectrum of peroxide radical  $(\text{OO})\text{CH}_2\text{OH}$  forming after matrix heating up to 115 K in the presence of oxygen.

of the methanol matrix. There is no full coincidence of these spectra. It is seen that the components of the triplet obtained by  $\text{IrCl}_6^{2-}$  photolysis contain an additional structure with the splitting of the order of 4–5 G. The longer irradiation is responsible for  $\text{}^1\text{CH}_2\text{OH}$  radical photolysis giving rise to  $\text{}^1\text{CH}_3$  and  $\text{HCO}^\bullet$  radicals [22]. At 77 K during half an hour the  $\text{}^1\text{CH}_3$  radicals convert again into  $\text{}^1\text{CH}_2\text{OH}$  [23]. Therefore, actually the  $\text{HCO}^\bullet$  radical is accumulated in the sample. The spectrum of  $\text{HCO}^\bullet$  is an asymmetric doublet with a splitting of about 130 G (Fig. 2).

Fig. 3 demonstrates the kinetic curves of  $\text{}^1\text{CH}_2\text{OH}$  and  $\text{HCO}^\bullet$  concentration increase, the disappearance of  $\text{IrCl}_6^{2-}$  complex and the appearance of the new optical absorption band with the maximum at 287 nm. All measurements (recording of optical and ESR spectra) were taken using the same sample. The solution was frozen in a flat quartz cuvette. The transparent glass obtained was uniformly irradiated by XeCl laser pulses (308 nm). After a definite number of pulses, the optical and ESR spectra were recorded. The  $\text{IrCl}_6^{2-}$  concentration was determined by the optical density of absorption band at 495 nm. The radical concentration was calculated by integrating the ESR spectra and calibrating against a standard, containing the  $\text{Cu}^{2+}$  ion ( $\text{CuCl}_2 \cdot 2\text{H}_2\text{O}$  single crystal).

As follows from Fig. 3, the concentration of  $\text{}^1\text{CH}_2\text{OH}$  first linearly increases with irradiation time, then passes through the maximum and begins to decrease. The  $\text{HCO}^\bullet$  radical emerges after a given induction period. Then its concentration increases and by the end of photolysis (complete disappearance of  $\text{IrCl}_6^{2-}$ ) it exceeds that of  $\text{}^1\text{CH}_2\text{OH}$  radical. Fig. 4 shows the ratio between the accumulated radicals concentration and the quantity of vanishing  $\text{IrCl}_6^{2-}$ . At large phototransformation depths, the total yield of radicals is less than 100%

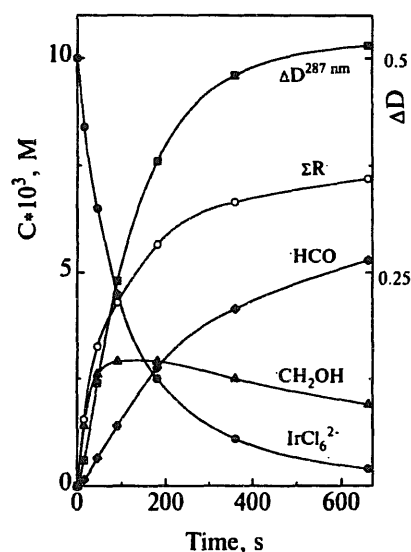


Fig. 3. Kinetic curves of the change in the concentration of different particles in  $\text{IrCl}_6^{2-}$  photolysis in methanol matrix (77 K) with the recording of optical and ESR spectra on the same sample (initial concentration of complex,  $1.0 \times 10^{-2}$  M; cuvette thickness, 0.033 cm; sample area,  $4.5 \times 11$  mm<sup>2</sup>, laser pulse energy, 3 mJ; repetition pulse frequency, 10 Hz).

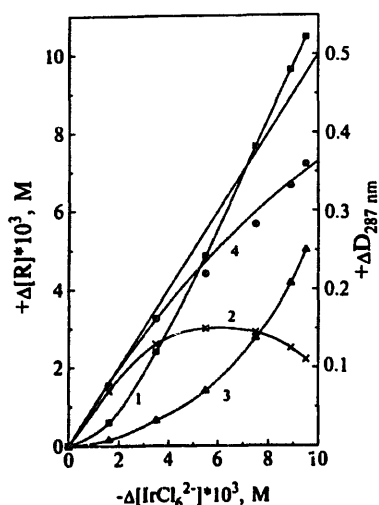


Fig. 4. Change in the concentration of different particles relative to the  $\text{IrCl}_6^{2-}$  concentration. Processing of Fig. 3 data. Curve 1 is the kinetics of the appearance of optical band with maximum at 287 nm. Curves 2–4 denote the  $\text{CH}_2\text{OH}$ ,  $\text{HCO}$ , and total radical concentration respectively. The straight line shows the hypothetical 100% total radicals yield.

and by the time  $\text{IrCl}_6^{2-}$  is completely photoreduced, it amounts to about 75%.

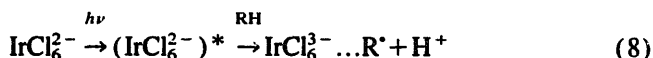
Thus, 25% of radicals can vanish in the reaction with  $\text{IrCl}_6^{3-}$  complex resulting in the formation of the  $\text{IrCl}_6^{4-}$  complex and, accordingly, of the new band with maximum at 287 nm. However, this reaction can be only the secondary photochemical reaction related to  $\text{CH}_2\text{OH}$  radical excitation because it occurs only under irradiation. If irradiation is interrupted once a given amount of  $\text{CH}_2\text{OH}$  has been accumulated, the radical concentration remains the same, and the optical density at 287 nm does not increase. An attempt to record the dark reaction of  $\text{CH}_2\text{OH}$  and  $\text{IrCl}_6^{3-}$  under laser flash photolysis of  $\text{IrCl}_6^{2-}$  methanol solution with large excess of  $\text{IrCl}_6^{3-}$  ( $10^{-2}$  M) at room temperature was not successful.

Fig. 4 shows the magnitude of optical density at 287 nm (with regard to the disappearance of  $\text{IrCl}_6^{2-}$  absorption at this wavelength). The curves allow calculation of extinction coefficient for this band, assuming it to belong to the  $\text{IrCl}_6^{4-}$  complex, the concentration of which is equal to the number of radicals being below 100%. Its value changes substantially with increasing phototransformation depth (from  $15 \times 10^3$  to  $7 \times 10^3 \text{ M}^{-1} \text{ cm}^{-1}$ ) which disagrees with the assumption that the band belongs to the  $\text{IrCl}_6^{2-}$  complex (extinction coefficient must be a constant). Besides, the values  $(15\text{--}7) \times 10^3 \text{ M}^{-1} \text{ cm}^{-1}$  considerably exceed that of  $1.7 \times 10^3 \text{ M}^{-1} \text{ cm}^{-1}$  given in Ref. [20]. For a given transformation depth, the band appears at 287 nm and the number of radicals still corresponds to that of disappearing  $\text{IrCl}_6^{2-}$ , which gives the overestimated values for the extinction coefficient. Thus, the probability of photochemical reaction between the  $\text{CH}_2\text{OH}$  radical and  $\text{IrCl}_6^{3-}$  is very low.

A decrease in the relative yield of radicals with increasing phototransformation depth can be assigned to radical recombination. In the rigid methanol matrix at 77 K there is no diffusion motion of alcohol radicals. However, a "light"

migration of valence is quite probable. For example, in the  $\text{FeCl}_3$  complex, if photolysis is performed in the methanol matrix under continued illumination of the sample, this process leads to the decrease of radical concentration according to the second-order kinetic law [4].

As for the photochemistry of Cu(II) and Pt(IV) chloride complexes and Mo(VI) oxocomplex [5–11], the appearance of band at 287 nm may be explained by the formation of a weakly bound charge transfer complex between radical and  $\text{IrCl}_6^{3-}$  ion



The appearance of charge transfer bands in either the nearest UV or the visible spectrum region is typical of such radical complexes. Thus, e.g. the  $\text{Cu(I)} \dots \text{R}^{\cdot}$  complexes exhibit absorption in the region 450–500 nm [5–7], those of the  $\text{Mo(V)} \dots \text{R}^{\cdot}$  at 500 nm [11], and for  $\text{Fe(II)} \dots \text{R}^{\cdot}$  the band appears at 280 nm [24]. A partial charge transfer is accompanied by spin density transfer from radical to complex. For the  $\text{Cu(I)} \dots \text{CH}_2\text{OH}$  complex the radical ESR spectrum is fully transformed and displays the anisotropic HFS on a copper nucleus (spin 3/2) [5]. According to estimates, the isotropic part of HFS ( $A_{\text{iso}}$ ) is determined by the transfer of the spin density on the copper nucleus 4s orbital [6].

For a copper atom the HFS constant (unpaired electron is fully situated on the 4s orbital) is about 2100 G [25]. The magnetic moment of copper nucleus is 14 times higher than that of the iridium one (spin of both natural isotopes  $^{191}\text{Ir}$  and  $^{193}\text{Ir}$  is 3/2 with almost identical magnetic moments). Therefore, in the case of full spin density transfer from radical to the iridium 6s orbital one should expect the lower HFS constants ( $A_{\text{iso}} < 160$  G). For the real spin density transfer of several percent (for  $\text{Cu(I)} \dots \text{CH}_2\text{OH}$   $\rho_{4s} \approx 0.05$  [6]) the isotropic splitting will be less than 8 G.

The anisotropic HFS ( $A_d$ ) on the iridium nucleus in the ESR spectrum can arise upon spin density delocalization from radical to 5d and 5p orbitals. In this case, the electron density can be transferred both from radical to ion and from ion to radical. The limiting case of full unpaired electron transfer from radical to iridium nucleus corresponds to the  $\text{Ir}^{2+}$  paramagnetic ion (5d<sup>7</sup> electron configuration). For the ion with such a configuration ( $\text{Ir}(\text{CN})_6^{4-}$  complex in the KCl single crystal) the anisotropic HFS constant  $A_d < 0.8$  G [26]. In the case of full electron density transfer from ion to radical the 5d<sup>5</sup> configuration appears. For this ion ( $\text{IrCl}_6^{2-}$  in  $\text{Na}_2\text{PtCl}_6 \cdot 6\text{H}_2\text{O}$  single crystal) the anisotropic constant is also small ( $A_d < 0.21$  G) [21]. For 5p electrons the anisotropic HFS is commonly even smaller [21]. Note that the isotropic constant for  $\text{Ir}^{4+}$  (5d<sup>5</sup> electrons) arises from the polarization of the inner ns electrons and is also rather low ( $A_{\text{iso}} \approx 25$  G).

These estimates show that upon partial spin density delocalization from radical to  $\text{IrCl}_6^{3-}$  one should expect only small HFS constants  $A_{\text{iso}}$  and  $A_d$  on the iridium nucleus. Theoretical calculations have shown the difficulty of reproducing the

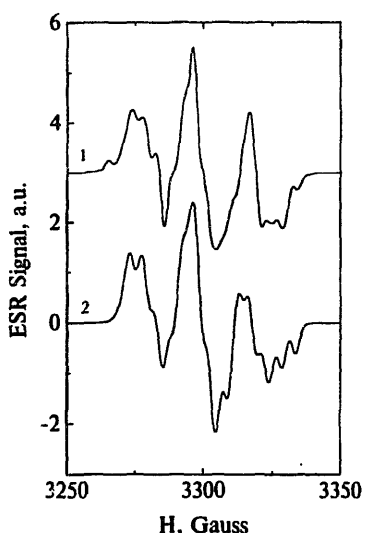


Fig. 5. Experimental (1) and calculated (2) ESR spectra of  $\text{IrCl}_6^{3-} \dots \text{CH}_2\text{OH}$  radical complex. Parameters of calculated spectrum:  $g$ -factors:  $g_x = 2.0043$ ;  $g_y = 2.0023$ ;  $g_z = 2.0003$ ; Linewidths:  $\Delta H_x = 5.0$ ;  $\Delta H_y = 5$ ;  $\Delta H_z = 1.2$  G; HFS on the first radical proton:  $A_x = 18$ ;  $A_y = 18$ ;  $A_z = 25$  G; HFS on the second radical proton:  $A_x = 16$ ;  $A_y = 16$ ;  $A_z = 19$  G; HFS on the iridium nucleus:  $A_x = 1$ ;  $A_y = 1$ ;  $A_z = 5$  G.

experimental spectrum completely. The general character of the spectrum is described only on the introduction of anisotropy of the  $g$ -factor, constants of splitting on radical protons, width of lines and splitting on an iridium nucleus. One of calculated spectra is shown in Fig. 5 with the parameters specified in drawing caption. The calculations were conducted with a Lorentzian line form. The introduction of isotropic parameters or the deviation of parameters by 10–20% considerably reduce the agreement of the calculated spectrum with the experimental one. The received values  $A_{\text{iso}}(\text{Ir}) \approx 2.33$  G and  $A_d(\text{Ir}) \approx 1.33$  G agree with the assumption of small spin density delocalization from radical to iridium 6s, 5d or 6p orbitals. Small non-equivalence of radical protons can be attributed to the radical complex structure.

It is assumed then that the novel band with maximum at 287 nm belongs to the radical complex  $\text{IrCl}_6^{3-} \dots \text{CH}_2\text{OH}$ . In this case, only the lower boundary can be given for the extinction coefficient of this band because the fraction of coordinated radicals is unknown. The existence of a small induction period in the appearance of this band can be explained by the appearance of radical complex in the secondary photochemical reaction. Laser irradiation at 308 nm falls within the wide  $\sigma_{\text{Cl}} \rightarrow 5d_{\text{Ir}}$  charge transfer band (with its maximum at 232 nm) of the  $\text{IrCl}_6^{2-}$  complex. The resulting ‘hole’ is localized on the  $\sigma_{\text{Cl}}$  orbitals of excited complex. Electron transfer and ‘hole’ filling occurs as the methanol molecules are in close contact with chlorine ions. In the rigid matrix the radical can occupy a more convenient position to form a radical complex due to valence transfer from the nearby molecule that is situated on the octahedron third-order axis, i.e. at the center of a regular triangle formed by three chlorine ions. Only in this position can the radical orbitals effectively be superimposed by those of the central ion. For such a

valence transformation to occur, a given number of radicals must be accumulated to capture part of the laser pulse quanta.

The radical photochemical activity manifests itself not only in its transformation within the second coordination sphere but also in the accumulation of  $\text{HCO}^\bullet$  radicals. This process is likely to be related to the valence transfer from the second coordination sphere to the matrix volume and the photodecomposition of  $^\bullet\text{CH}_2\text{OH}$  radical. The  $\text{HCO}^\bullet$  radicals can be converted back into  $^\bullet\text{CH}_2\text{OH}$  (by irradiating the sample by light with  $\lambda > 530$  nm) without changing the total concentration of these particles [23]. Assuming that at the end of photolysis all  $^\bullet\text{CH}_2\text{OH}$  radicals are bound in the complex with  $\text{IrCl}_6^{3-}$ , the band extinction coefficient of the radical complex at 287 nm is  $\geq 8 \times 10^3 \text{ M}^{-1} \text{ cm}^{-1}$ .

In addition to the band at 287 nm, the  $\text{IrCl}_6^{3-} \dots \text{CH}_2\text{OH}$  complex can have the absorption in the more short-wave region of the spectrum. Superposition of the  $\text{IrCl}_6^{3-}$  and  $\text{IrCl}_6^{3-} \dots \text{CH}_2\text{OH}$  spectra is likely to cause the shift of the absorption maximum of photolysis products from 211 nm ( $\text{IrCl}_6^{3-}$ ) to 215 nm.

### 3.3. Disappearance of $\text{IrCl}_6^{3-}$ photolysis products with increasing temperature of methanol matrix

Fig. 6 shows the decrease of relative radical concentration with increasing matrix temperature. The sample was heated at each point for 10 min and then frozen to 77 K. Then the ESR spectrum was recorded. The temperature behavior of optical spectra was studied by the same method. To transform

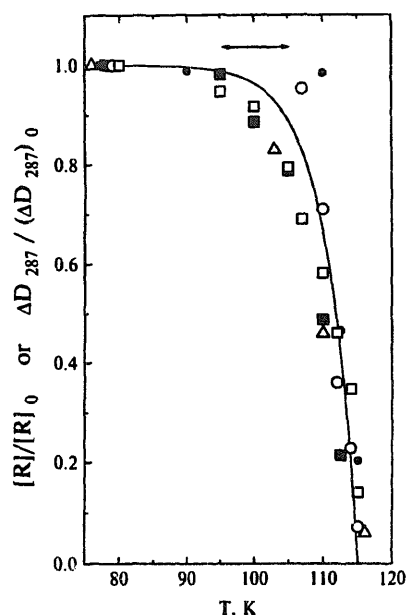


Fig. 6. The annealing of  $\text{IrCl}_6^{3-}$  photolysis products in methanol matrix (10 min at each temperature).  $\circ$ ,  $\square$  denote the dependence of radical concentration on temperature for photolyzed and  $\gamma$ -radiolyzed oxygen free samples;  $\bullet$ ,  $\blacksquare$  show the same dependence for photolyzed and  $\gamma$ -radiolyzed natural oxygen samples, respectively (before annealing the  $\text{HCO}^\bullet$  radicals were converted into  $^\bullet\text{CH}_2\text{OH}$  by irradiating the sample with light at  $\lambda > 530$  nm).  $\Delta$  denotes the change in the 287 nm band intensity. The arrow shows the range of  $^\bullet\text{CH}_2\text{OH} \rightarrow (\text{OO})\text{CH}_2\text{OH}$  transformation.

the  $\text{HCO}^\bullet$  radical to the  $\text{CH}_2\text{OH}^\bullet$  one, the samples were irradiated with light at  $\lambda > 530$  nm. The total radical concentration, in this case, remained constant. Fig. 6 shows also the temperature dependence of optical density at 287 nm (relative to the optical density at 77 K) and the behavior of ESR spectrum of  $\text{CH}_2\text{OH}^\bullet$  radicals obtained by the  $\gamma$ -radiolysis of methanol matrix.

As follows from Fig. 6, both the lines in the ESR spectrum and the band at 287 nm simultaneously vanish with rising temperature. The primary photolysis products begin to disappear at approximately 109 K, i.e. near the glass transition point of methanol matrix. When the temperature is about 115 K, more than 90% of particles disappear. A simultaneous disappearance of both radicals and optical band at 287 nm confirms its relation to radical stabilization in the second coordination sphere of the  $\text{IrCl}_6^{3-}$  complex.

For the  $\text{Cu(I)} \dots \text{R}^\bullet$  radical complex in alcohol matrices the temperature range of decay is shifted by 10 K towards higher temperatures in comparison with the disappearance of a free noncoordinated radical  $\text{R}^\bullet$  [5]. Using laser flash photolysis it has been established [7] that at 140 K (above glass transition temperature but below melting point) these radical complexes vanish during 100  $\mu\text{s}$ . The extrapolation of temperature dependence shows that at room temperature the decay time is shorter than 30 ns [7]. Thus, the  $\text{Cu(I)} \dots \text{R}^\bullet$  complexes are the unstable systems that decompose into the complex ion of  $\text{Cu(I)}$  and free radical  $\text{R}^\bullet$ . A fast dissociation is also typical of the radical complex  $\text{Pt(III)} \dots \text{R}^\bullet$  (20 ns at room temperature [9]).

For the  $\text{IrCl}_6^{2-} \dots \text{CH}_2\text{OH}^\bullet$  complex the temperature region of decay is practically unshifted relative to the region of free radicals decay (Fig. 6). This complex dissociates just after the glass transition point during the unfreezing of diffusion mobility of particles in the matrix.

The  $\text{CH}_2\text{OH}^\bullet$  radicals resulting from  $\gamma$ -irradiation of the methanol matrix usually recombine to form ethylene glycol [27]. In our case, if irradiation is stopped at the instant when there is still a sufficient amount of the initial  $\text{IrCl}_6^{2-}$  complex (e.g. 50%), the heating of matrix leads to the additional decrease of the optical density of the  $\text{IrCl}_6^{2-}$  absorption bands. This decrease is determined by the reaction of  $\text{CH}_2\text{OH}^\bullet$  radicals with  $\text{IrCl}_6^{2-}$ . The rate constant of this reaction is close to that of radical recombination ( $3 \times 10^9$  [1] and  $1.4 \times 10^9 \text{ M}^{-1} \text{ s}^{-1}$  [27] at room temperature, respectively). Thus, the reaction between  $\text{CH}_2\text{OH}^\bullet$  and  $\text{IrCl}_6^{2-}$  with increasing matrix temperature also testifies to the fast dissociation of the radical complex  $\text{IrCl}_6^{2-} \dots \text{R}^\bullet$  followed by radical escape into the bulk.

As has been mentioned, the optical absorption band with the maximum at 280 nm belonging, probably, to the complex of divalent iridium,  $\text{IrCl}_6^{4-}$ , has been recorded under pulsed radiolysis of the aqueous solutions of  $\text{IrCl}_6^{3-}$  with *t*-butanol impurities [20]. However, there is an alternative explanation for the nature of this band. When the *t*-butanol concentration is high (0.1–0.5 M) the primary products of water radiolysis ( $\text{OH}^\bullet$  radicals) rapidly convert *t*-butanol into *t*-butanol radi-

icals,  $\text{CH}_2(\text{CH}_3)_2\text{COH}^\bullet$ . In the frame of the above concepts developed for  $\text{IrCl}_6^{2-}$  photochemistry, the *t*-butanol radicals can form a radical complex  $\text{IrCl}_6^{2-} \dots \text{CH}_2(\text{CH}_3)_2\text{COH}^\bullet$  with  $\text{IrCl}_6^{2-}$  ion. The band with the maximum at 280 nm observed under pulsed radiolysis can belong just to this particle.

#### 3.4. Annealing of $\text{IrCl}_6^{2-}$ photolysis products in the presence of oxygen

One of the channels for disappearance of the primary radical complexes  $\text{Cu(I)} \dots \text{R}^\bullet$  and  $\text{Pt(III)} \dots \text{R}^\bullet$  in the presence of oxygen in the matrix is their transformation into the secondary complexes  $\text{Cu(I)} \dots \text{RO}_2^\bullet$  and  $\text{Pt(III)} \dots \text{RO}_2^\bullet$  that display the optical absorption bands [9,28]. When methanol matrices containing oxygen ( $2.6 \times 10^{-3} \text{ M}$ ) are heated after  $\text{IrCl}_6^{2-}$  is photoreduced, the disappearance of the band with maximum at 287 nm does not produce optical absorption bands within the range 280–800 nm. In the ESR spectrum the  $\text{CH}_2\text{OH}^\bullet$  radical lines transform into the new spectrum with an axial anisotropic *g*-factor. This spectrum (Fig. 2, spectrum 4) belongs to the peroxide radical  $(\text{OO})\text{CH}_2\text{OH}^\bullet$  [29]. The identical spectrum can be obtained by heating a  $\gamma$ -radiolyzed methanol matrix containing oxygen. Fig. 6 depicts the temperature dependence of radical concentration for the matrix with oxygen for both the photolyzed sample with  $\text{IrCl}_6^{2-}$  and the  $\gamma$ -radiolyzed matrix. Thus, the radical complex  $\text{IrCl}_6^{2-} \dots \text{CH}_2\text{OH}^\bullet$  dissociates faster than its reaction with oxygen can occur.

## 4. Conclusions

The present paper demonstrates that the photoreduction of  $\text{IrCl}_6^{2-}$  in a frozen methanol matrix as well as in solutions is caused by electron transfer from surrounding molecules to the excited complex. The  $\text{IrCl}_6^{3-}$  and  $\text{CH}_2\text{OH}^\bullet$  particles forming in the primary process give rise to the radical complex  $\text{IrCl}_6^{3-} \dots \text{R}^\bullet$  that displays the optical absorption band with maximum at 287 nm. In the ESR spectrum the coordination of  $\text{CH}_2\text{OH}^\bullet$  radicals manifests itself in the additional splitting, probably, due to the partial delocalization of spin density to the orbitals of the central ion  $\text{Ir(III)}$  (iridium nucleus spin is 3/2). When the matrix is heated in the region 110–115 K, the optical band at 287 nm and the ESR spectrum of radicals and radical complexes decay. Thus, at low temperatures the primary radicals form weakly bound complexes with a photoreduced metal ion in the photochemistry of  $\text{Cu(II)}$ ,  $\text{Mo(VI)}$ ,  $\text{Pt(IV)}$  and  $\text{Ir(IV)}$  complexes.

## Acknowledgements

The work was supported by RFFI (grants 94-03-08633, 96-03-33495) and the Competition Center at the Saint-Peterburg University (grant 94-9.2-108). The authors also thank

Dr. A. Shubin for the placing at our disposal the computer program of ESR spectra calculation.

## References

- [1] E.M. Glebov, V.F. Plyusnin, N.I. Sorokin, V.P. Grivin, A.B. Venediktov, H. Lemmetyinen, *J. Photochem. Photobiol. A: Chem.* 90 (1995) 31.
- [2] I.V. Khmelinskii, V.F. Plyusnin, V.P. Grivin, *Zh. Fiz. Khim.* 53 (1989) 2722.
- [3] I.V. Khmelinskii, V.F. Plyusnin, V.P. Grivin, *Khim. Vys. Energ.* 22 (1988) 239.
- [4] V.F. Plyusnin, N.M. Bazhin, *Khim. Vys. Energ.* 15 (1981) 142.
- [5] V.F. Plyusnin, N.M. Bazhin, O.B. Kiseleva, *Khim. Vys. Energ.* 12 (1978) 87.
- [6] N.P. Gritsan, O.M. Usov, N.V. Shokhirev, I.V. Khmelinskii, V.F. Plyusnin, N.M. Bazhin, *Teor. Eksp. Khim.* 21 (1986) 31.
- [7] I.V. Khmelinskii, V.F. Plyusnin, N.P. Gritsan, N.M. Bazhin, *Khim. Fiz.* 4 (1985) 1666.
- [8] V.P. Grivin, I.V. Khmelinskii, V.F. Plyusnin, I.I. Blinov, K.P. Balashev, *J. Photochem. Photobiol. A: Chem.* 51 (1990) 167.
- [9] V.P. Grivin, I.V. Khmelinskii, V.F. Plyusnin, *J. Photochem. Photobiol. A: Chem.* 51 (1990) 379.
- [10] V.P. Grivin, I.V. Khmelinskii, V.F. Plyusnin, *J. Photochem. Photobiol. A: Chem.* 59 (1991) 153.
- [11] S.Ya. Kuchmii, T.I. Serdyukova, A.I. Kryukov, *Teor. Eksp. Khim.* 18 (1982) 578.
- [12] E.N. Sloth, C.S. Garner, *J. Am. Chem. Soc.* 77 (1955) 1440.
- [13] V.V. Korolev, V.F. Plyusnin, N.M. Bazhin, *Zh. Fiz. Khim.* 49 (1975) 2440.
- [14] C.K. Jorgensen, *Mol. Phys.* 2 (1959) 309.
- [15] P. Day, C.K. Jorgensen, *Chem. Phys. Lett.* 1 (1968) 507.
- [16] A.I. Kryukov, L.V. Nazarova, B.Ya. Dain, *Ukr. Khim. Zh.* 29 (1963) 812.
- [17] O. Hinojos, J.A. Harris, J.C. Arthur, *Carbohydr. Res.* 41 (1975) 31.
- [18] F.S. Dainton, G.A. Salmon, P. Wardman, *Proc. R. Soc. Lond.*, A313 (1969) 1.
- [19] M. Simic, P. Neta, E. Hayon, *J. Phys. Chem.* 73 (1969) 3794.
- [20] R.K. Broszkiewich, *J. Chem. Soc., Dalton Trans.* 17 (1973) 1799.
- [21] J. Owen, K.W.H. Stevens, *Nature (London)* 171 (1953) 836.
- [22] S.B. Milliken, R.H. Johnson, *J. Phys. Chem.* 71 (1967) 2116.
- [23] B.N. Shelimov, N.V. Fok, V.V. Voevodski, *Kinet. i Katal.* 4 (1963) 539.
- [24] A.G. Pribush, S.P. Brusentsova, V.N. Shubin, P.I. Dolin, *Khim. Vys. Energ.* 9 (1975) 235.
- [25] P.H. Kasai, D. McCleod, *J. Chem. Phys.* 55 (1971) 1566.
- [26] N.V. Vugman, R.P.A. Muniz, J. Danon, *J. Chem. Phys.* 57 (1972) 1297.
- [27] D.W. Johnson, G.A. Salmon, *Can. Chem. J.* 55 (1977) 2030.
- [28] N.P. Gritzan, V.F. Plyusnin, N.M. Bazhin, *Teor. Exper. Khim.* 21 (1986) 39.
- [29] E.A. Zapadinski, V.A. Tolkathev, *Khim. Vys. Energ.* 22 (1988) 305.